ELSEVIER

Applied Catalysis A: General 213 (2001) 279–288

APPLIED CATALYSIS A: GENERAL

www.elsevier.com/locate/apcata

An XPS study of dispersion and chemical state of MoO_3 on Al_2O_3-TiO_2 binary oxide support

Benjaram M. Reddy [a,*], Biswajit Chowdhury [a], Ettireddy P. Reddy [a,b], Asunción Fernández [b]

[a] *Inorganic and Physical Chemistry Division, Indian Institute of Chemical Technology, Hyderabad 500007, India*
[b] *Instituto de Ciencia de Materiales de Sevilla, Centro de Investigaciones Científicas, Isla de la Cartuja, Avda. Américo Vespucio s/n, 41092 Sevilla, Spain*

Received 9 October 2000; received in revised form 14 December 2000; accepted 15 December 2000

Abstract

X-ray photoelectron spectroscopy (XPS) technique was employed to characterize Al_2O_3-TiO_2 support and MoO_3/Al_2O_3-TiO_2 catalyst calcined at different temperatures from 773 to 1073 K. The Al_2O_3-TiO_2 (1:1.3 mole ratio) binary oxide support was obtained by a coprecipitation procedure with in situ generated ammonium hydroxide. A nominal 12 wt.% MoO_3 was impregnated over the calcined (773 K) support by a wet impregnation method. The initial characterization by X-ray powder diffraction, Fourier transform-infrared (FT-IR), and O_2 chemisorption techniques revealed that the impregnated MoO_3 is in a highly-dispersed state on the surface of the support. XPS electron binding energy (E_b) values indicate that the MoO_3/Al_2O_3-TiO_2 catalyst contains the mixed-oxide elements in the highest oxidation states, Ti(IV), Al(III), and Mo(VI), respectively. However, the core level E_b of Al 2p slightly increased with increase of calcination temperature, and this effect was more prominent in the case of molybdena-doped samples. A better resolved Mo 3d doublet was observed at all calcination temperatures. This was explained as due the coverage of alumina surface by titania, thereby lowering the interaction between molybdena and alumina. The XPS atomic ratios indicate that the Ti/Al ratio is sensitive to the calcination temperature. The Mo/Al ratio was found to be more than that of Mo/Ti ratio and decreased with increasing calcination temperature. A clear difference between the Al_2O_3 and the TiO_2 surfaces, in terms of surface free energy, isoelectric point, and surface hydroxyl distribution was considered to be responsible for different distributions of molybdena over these supports.

Keywords: Molybdena; Al_2O_3-TiO_2; MoO_3/Al_2O_3-TiO_2; Mixed oxide; XPS; XRD; Dispersion; Thermal stability

1. Introduction

Supported-molybdenum oxide catalysts are widely used in various catalytic processes. The molecular structure of molybdenum oxide on different supports has also been extensively investigated by various techniques over the past decade [1,2]. Several studies in the literature employing Raman, Fourier transform-infrared (FT-IR), solid state ^{95}Mo nuclear magnetic resonance (NMR), extended X-ray absorption fine structure (EXAFS), X-ray absorption near edge structure (XANES), X-ray photoelectron spectroscopy (XPS), and ultraviolet visible diffuse reflectance spectroscopies (UV-DRS) have concluded that the surface structure of supported-molybdenum

* Corresponding author. Fax: +91-40-717-3387.
E-mail address: bmreddy@iict.ap.nic.in (B.M. Reddy).

0926-860X/01/$ – see front matter
PII: S0926-860X(00)00906-6

oxide is highly sensitive to the nature of support, molybdenum oxide loading, extent of surface hydration and dehydration, surface impurities, and calcination temperature [3–16]. In particular, the structure of molybdenum oxide/sulfide on alumina support has been extensively studied under ambient, dehydrated, and reaction conditions [2,11, 14–16].

Besides alumina, there has been an increasing amount of interest over the past few years on other supports, such as titania, zirconia, ceria, and activated carbon. Molybdena-titania combination is an excellent catalyst or catalyst precursor for gas–oil hydrotreatment [17], alkene metathesis [18], and selective oxidation of hydrocarbons [19]. For example, the intrinsic activity of Mo atom on TiO_2 was 1.5 times more than that on the Al_2O_3 support for hydrogenation of a model reaction, tetralin [20]. However, a major disadvantage associated with TiO_2 support is its low specific surface area and low thermal stability of the active anatase structure at high temperatures. To overcome these deficiencies, titania was combined with alumina or silica, by taking advantage of the high thermal stability of Al_2O_3 or SiO_2 to stabilize the specific surface area and the structure of anatase. A few studies concerning the structural and catalytic properties of TiO_2-Al_2O_3 mixed oxides have been reported [20–26]. For example, the MoO_3 when supported on TiO_2-Al_2O_3 was found to exhibit better catalytic performance for hydrodesulfurization reaction [22].

The primary objective of this study was to follow the structure evaluation of Al_2O_3-TiO_2 mixed oxide support and the dispersion and nature of molybdenum oxide phase on this support under the influence of thermal treatments. X-ray photoelectron spectroscopy (XPS or ESCA), because of its high surface sensitivity (probing depth ca. 2 nm), has been considered as one of the best techniques for studying the dispersion of transition metal oxides on various supports and to gain knowledge on the type of interaction involved between the active metal oxide species and the supporting oxide [27–30]. In the present investigation, the XPS technique was applied to get more information on the preferential interaction of molybdenum oxide with alumina and/or titania components of the binary oxide support.

2. Experimental

2.1. Catalyst preparation

The Al_2O_3-TiO_2 (1:1.3 mole ratio) support was prepared by a homogeneous coprecipitation method with in situ generated ammonium hydroxide by decomposition of urea at 368 K. To achieve this, a mixed aqueous solution of $NaAlO_2$ (Loba Chemie, GR grade), $TiCl_4$ (Fluka, AR grade), and urea (Loba Chemie, GR grade) was heated to 368 K with vigorous stirring. In about 6 h of heating, as decomposition of urea progressed to a certain extent, the formation of precipitate gradually occurred. The precipitate was heated for 6 h more to facilitate aging. Thus, formed coprecipitate was filtered-off, washed several times with deionized water until free from chloride ions, and dried at 393 K for 16 h. To remove residual sodium ions, the oven-dried precipitates were again washed with ammonium nitrate solution (5%) several times, followed by hot distilled water, and dried once again at 383 K for 12 h. The obtained sample was finally calcined at 773 K for 6 h in open-air atmosphere. Some portions of this finished Al_2O_3-TiO_2 support were once again heated at 873, 973, and 1073 K for 6 h in a closed electrical furnace in open-air atmosphere.

To make MoO_3/Al_2O_3-TiO_2 catalyst, a nominal 12 wt.% MoO_3 was deposited on the Al_2O_3-TiO_2 support by a standard wet impregnation method. To impregnate MoO_3, the requisite quantity of ammonium heptamolybdate (JT Baker, UK, AR grade) was dissolved in doubly-distilled water, and the finely-powdered calcined (773 K) mixed oxide support was added to this solution. The excess water was evaporated on a water bath with continuous stirring. The resultant solid was then dried at 383 K for 12 h and calcined at 773 K for 6 h in a closed electrical furnace in open-air atmosphere. Some portions of the finished catalyst were once again heated at 873, 973, and 1073 K for 6 h in a closed electrical furnace in open-air atmosphere. The rate of heating (as well as cooling) was always maintained at 10 K min^{-1}.

2.2. Catalyst characterization

X-ray powder diffraction patterns have been recorded on a Siemens D-5000 diffractometer by using Cu Kα radiation source. The XRD phases present in

the samples were identified with the help of JCPDS files. The X-ray line broadening technique was used to determine the crystallite size of TiO_2 anatase in the samples from XRD data of (1 0 1) reflection. The FT-IR spectra were recorded on a Nicolet 740 FT-IR spectrometer at ambient conditions using KBr discs with a nominal resolution of $4\,cm^{-1}$ and averaging 1 0 0 spectra. Oxygen chemisorption measurements were made as per the procedure described elsewhere [31].

The XPS measurements were made on a VG Scientific ESCA Lab 210 spectrometer. The Mg Kα and Al Kα radiations were used as excitation sources. The spectra were recorded in the fixed analyzer transmission mode, the pass energy being 50 eV. The scanning of the spectra was done at pressures less 10^{-8} Torr. The Ti $2p_{3/2}$ or C 1s lines were taken as internal references with a binding energy of 458.5 and 285.0 eV, respectively [32]. An estimated error of ±0.1 eV can be assumed for all the measurements. Quantitative analysis of atomic ratios was accomplished by determining the elemental peak areas, following a Shirley background subtraction by the usual procedures [32–34], and carried out using the sensitivity factors supplied with the instrument. The modified Auger parameter of Ti and Al was calculated according to the following equations:

$$\alpha^{I}(\mathrm{Ti}) = \alpha + h\nu = \mathrm{BE\ of\ the\ Ti\ 2p_{3/2}\ peak} + \mathrm{KE\ of\ the\ Ti\ L_3M_{23}V\ Auger\ peak}$$

$$\alpha^{I}(\mathrm{Al}) = \alpha + h\nu = \mathrm{BE\ of\ the\ Al\ 2p\ peak} + \mathrm{KE\ of\ the\ Al\ KL_{23}L_{23}\ Auger\ peak}$$

where BE is the binding energy and KE the kinetic energy [35,36].

3. Results and discussion

The alumina-titania binary oxide support calcined at 773 K exhibited a specific surface area of $159\,m^2\,g^{-1}$. Therefore, a 12 wt.% MoO_3 was selected to impregnate over the support surface to achieve a monolayer coverage [37,38]. The X-ray powder diffraction analysis of MoO_3/Al_2O_3-TiO_2 catalyst (773 K) also revealed that there are no XRD lines due to crystalline MoO_3, except the broad diffraction lines due to TiO_2 anatase. The FT-IR spectra of the sample also supported the XRD observations. The O_2 chemisorption measurements obtained as per the procedure described elsewhere [31] also revealed that the MoO_3 is in a highly-dispersed state on the support surface at 773 K calcination temperature. Chemisorption of O_2 is possible only on the reduced Mo oxide, which contains coordinately-unsaturated sites. The O_2 chemisorption method discriminates between the monolayer and crystalline Mo oxide phases, since their reduction behaviors are entirely different [39]. The preliminary characterization results thus suggest that the impregnated molybdena is in a highly-dispersed state on the surface of the Al_2O_3-TiO_2 support. In other words, there is no excess MoO_3 in the microcrystalline form on the Al_2O_3-TiO_2 carrier when calcined at 773 K.

To understand the temperature stability of the Al_2O_3-TiO_2 support and the MoO_3/Al_2O_3-TiO_2 catalyst, samples were subjected to high temperature treatments from 773 to 1073 K. The BET surface area of the Al_2O_3-TiO_2 support was found to decrease from $159\,m^2\,g^{-1}$ at 773 K to $32\,m^2\,g^{-1}$ at 1073 K due to sintering. The sintering effect was little larger in the case of molybdena-impregnated samples. The BET surface area of the 12% MoO_3/Al_2O_3-TiO_2 catalyst was observed to decrease from $96\,m^2\,g^{-1}$ at 773 K to $26\,m^2\,g^{-1}$ at 1073 K. The XRD patterns of Al_2O_3-TiO_2 exhibited only anatase phase, and the intensity of the lines due to this phase was observed to increase with increasing calcination temperature. The crystallite size of anatase increased from ca. <3.5 nm at 773 K to 15.1 nm at 1073 K. There is no evidence in the literature about the existence of solid solutions between alumina and titania. However, the formation of only one definite compound Al_2TiO_5 was reported above 1273 K temperature [40]. The dispersed MoO_3, in the case of MoO_3/Al_2O_3-TiO_2 catalysts, was found to exhibit some influence on the crystallization of anatase. The crystallite size of anatase increased from 5.1 nm at 773 K to 18.6 nm at 1073 K. Some broad diffraction lines due to $Al_2(MoO_4)_3$ compound together with TiO_2 rutile lines were noted at 1073 K.

The samples of Al_2O_3-TiO_2 and MoO_3/Al_2O_3-TiO_2 calcined at different temperatures have been investigated by XPS technique. The photoelectron peaks of O 1s, Ti 2p, Al 2p, and Mo 3d are presented in Figs. 1, 2, 3 and 4, respectively. For the purpose of better comparison, the XPS photoelectron peaks of

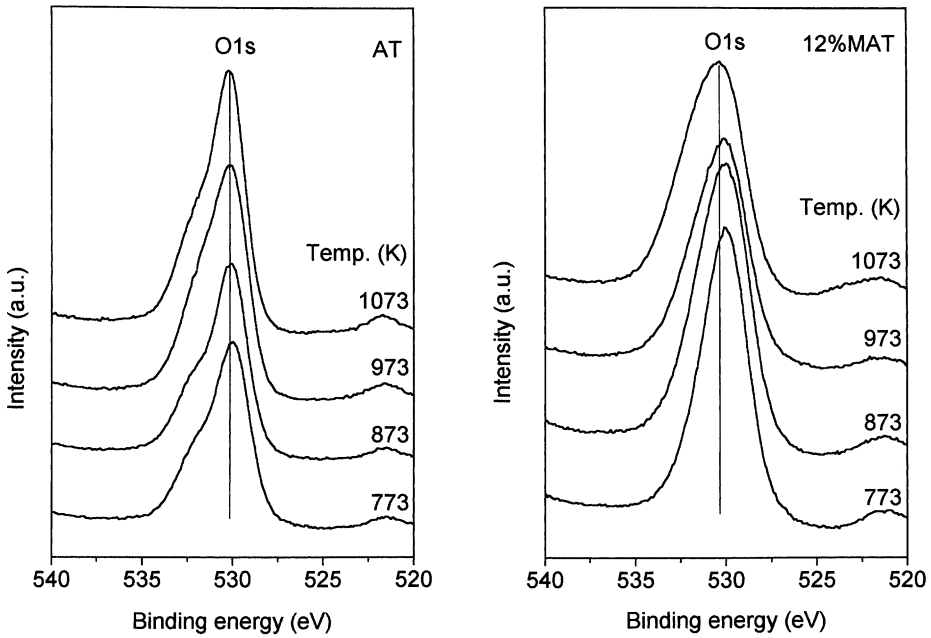

Fig. 1. XPS of the O 1s binding energy region for Al_2O_3-TiO_2 (AT) support and MoO_3/Al_2O_3-TiO_2 (12% MAT) catalyst calcined at different temperatures.

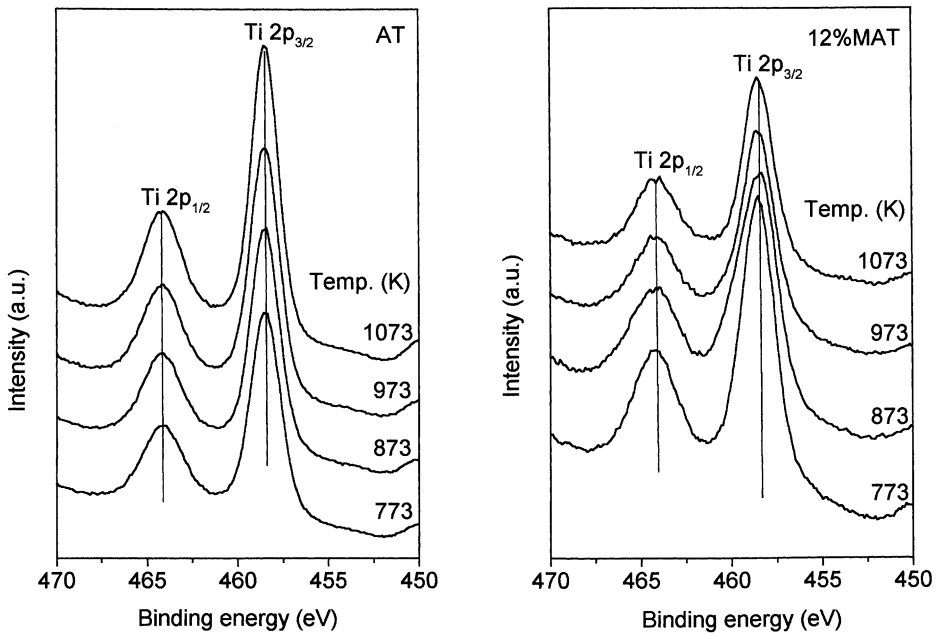

Fig. 2. Ti 2p XPS spectra of Al_2O_3-TiO_2 (AT) support and MoO_3/Al_2O_3-TiO_2 (12% MAT) catalyst calcined at different temperatures.

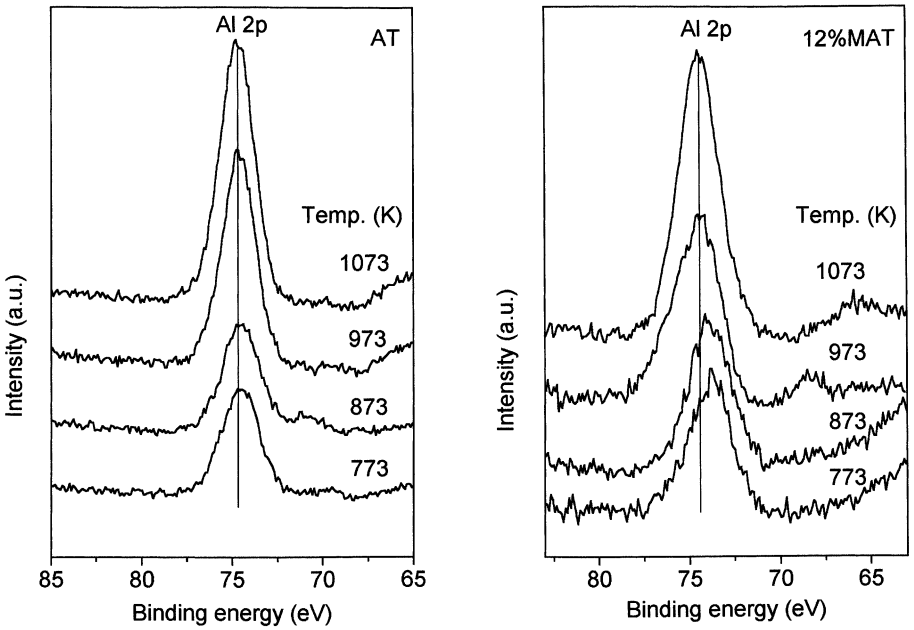

Fig. 3. Al 2p XPS spectra of Al_2O_3-TiO_2 (AT) support and MoO_3/Al_2O_3-TiO_2 (12% MAT) catalyst calcined at different temperatures.

O 1s, Ti 2p, and Al 2p pertaining to the Al_2O_3-TiO_2 binary oxide support and the corresponding peaks of the MoO_3/Al_2O_3-TiO_2 catalyst are shown together in these figures. The corresponding electron binding energies (E_b) and the Auger parameter values are presented in Table 1. In general, the intensity of all photoelectron peaks increased with increasing calcination temperature. This general effect is also accompanied by a diminution of C 1s peak intensity, which indicates clearly that the calcination treatment is also cleaning the surface of the samples from carbon contamination. The O 1s profile (Fig. 1) is, in general, complicated due to the overlapping contribution of oxygen from titania and alumina in the case of the Al_2O_3-TiO_2 support and from titania, alumina, and molybdena in the case of the MoO_3/Al_2O_3-TiO_2 catalyst. Two oxygen peaks are observed for the Al_2O_3-TiO_2 support at all calcination temperatures. The O 1s line with E_b = 530.0–530.4 eV can be assigned to the lattice oxygen of the TiO_2. The second O 1s line at higher binding energy (E_b = 531.1–531.4 eV) is due to Al_2O_3. This assignment is easily possible judging from the difference in the electronegativity of the elements involved [41] and also from the literature [42]. Overlapping contribution from molybdena made it difficult to discriminate the different oxygen peaks in the case of the MoO_3/Al_2O_3-TiO_2 catalyst. The pure MoO_3 exhibits a sharp O 1s peak at E_b = 530.62 [43]. In the case of the Al_2O_3-TiO_2 carrier, the

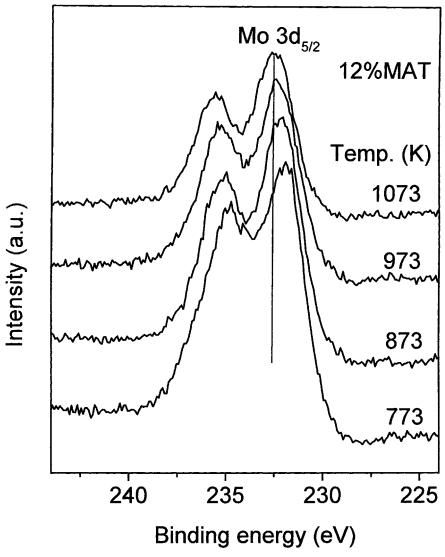

Fig. 4. Mo 3d XPS spectra of MoO_3/Al_2O_3-TiO_2 (12% MAT) catalyst calcined at different temperatures.

Table 1
Electron binding energies (E_b), modified Auger parameter values, and XPS atomic ratios for Al_2O_3-TiO_2 support and 12 wt.% MoO_3/Al_2O_3-TiO_2 catalyst calcined at different temperatures[a]

Temperature (K)	Ti $2p_{3/2}$	Ti KE	α^I (Ti)	Al 2p	Al KE	α^I (Al)	O 1s	Mo $3d_{5/2}$	Ti/Al	Mo/Ti	Mo/Al
Al_2O_3-TiO_2 support											
773	458.5	414.6	873.1	74.5	1387.5	1462.0	530.0		2.58		
873	458.5	414.7	873.2	74.6	1387.4	1462.0	530.1		2.02		
973	458.5	414.6	873.1	74.6	1387.2	1461.8	530.1		1.57		
1073	458.5	414.7	873.2	74.7	1387.0	1461.7	530.2		1.20		
MoO_3/Al_2O_3-TiO_2 catalyst											
773	458.5	415.0	873.5	74.2	1388.2	1462.4	530.0	232.1	1.67	0.31	0.37
873	458.5	415.1	873.6	74.5	1387.7	1462.2	530.3	232.3	1.16	0.30	0.35
973	458.5	415.3	873.8	74.6	1387.3	1461.9	530.6	232.6	1.00	0.28	0.33
1073	458.5	415.4	873.9	74.8	1386.7	1461.5	530.7	232.7	0.48	0.25	0.18

[a] All values are in electron volts, eV, except atomic ratios.

binding energy of the most intense O 1s peak (Table 1) is almost constant with increase of calcination temperature. However, a clear increase in the binding energy of the O 1s peak with temperature is observed for molybdena-doped samples. This may be due to the segregation of molybdenum oxide on the support surface or the formation of $Al_2(MoO_4)_3$ compound with increase of calcination temperature [15].

Fig. 2 shows the Ti 2p photoelectron peaks at E_b = 458.5 and 464.4 eV for Ti $2p_{3/2}$ and Ti $2p_{1/2}$ lines, respectively, which agree well with values reported in the literature [41,44,45]. It is interesting to note that the intensity of the Ti 2p core level spectra, in the case of Al_2O_3-TiO_2 mixed oxide, increased with increasing calcination temperature. This may be due to two reasons: the first one is the elimination of residual carbon during calcination of the samples in air at higher temperatures, and the other one is the crystallization of titania with increase of calcination temperature as observed from XRD studies. The Auger parameter for Ti has also been measured and summarized in Table 1. A small but insignificant variation can be seen for all the samples. As this parameter does not depend on charge effects, Ti seems to be in a similar chemical state in all the samples. Therefore, Ti was considered as a good reference for binding energy calibrations [36,45,46]. The results thus suggest that the titania in the Al_2O_3-TiO_2 support and in the MoO_3/Al_2O_3-TiO_2 catalyst is in the highest oxidation state of Ti(IV) irrespective of high temperature treatments.

Fig. 3 shows the Al 2p photoelectron peak of the samples calcined at various temperatures. The corresponding binding energies and the Auger parameter values are shown in Table 1. An insignificant slight increase in the core level E_b and decrease in the Auger parameter value can be noted with increasing calcination temperature. These changes in the binding energy (E_b = 74.2–74.8 eV) and the Auger parameter value (α^I = 1462.4–1461.5 eV) are slightly larger in the case of MoO_3/Al_2O_3-TiO_2 catalyst, in comparison to the pure support (E_b = 74.5–74.7 eV and α^I = 1462.0–1461.7 eV). The slight increase in binding energy and decrease in Auger parameter values may be explained to be due to the disappearance of the surface hydroxyl groups of the alumina support. On thermal treatment, water is normally evolved from two neighboring hydroxyl ions which leave the coordination sphere of an aluminum ion incomplete. So, there is a removal of negative charge density from the alumina center due to dehydroxylation, which has been reflected in the binding energy. Dehydroxylation is more in the case of molybdena-doped samples due to formation of Mo–O–Al bonds during calcination by exchange of surface hydroxyl groups between the active component and the support [14,15,47]. As per the literature, there is also a small increase in the E_b of Al 2p during transformation of Al_2O_3 from γ- to the α-phase under the influence of thermal treatments beyond 873 K [48]. However, the XRD technique failed to detect the lines due to α-Al_2O_3 phase in the samples calcined up to 1073 K due to poor crystallinity of this phase. However, its presence was noted at 1273 K calcination. An increase in the E_b of Al 2p was also noted due to the formation of $Al_2(MoO_4)_3$ between

Al_2O_3 and MoO_3 oxides [49]. These observations reveal that the alumina in the mixed oxide may probably convert partially from the metastable gamma to the stable alpha phase in the case of pure support, and to a definite $Al_2(MoO_4)_3$ compound in the case of MoO_3/Al_2O_3-TiO_2 catalyst at higher calcination temperatures. As reported in the literature, the Auger parameter is known to provide information about the electronic properties of the oxides dispersed on metal or metal oxides [35,46]. The binding energy and the Auger parameter of TiO_2 deposited on SiO_2 have been changed by 0.7 and 2.6 eV as the coverage increases [36]. The observed small variation in the binding energy and the Auger parameter value of aluminum in comparison to titanium indicate that the former might have been modified due to the influence of the TiO_2 support. To establish this fact, further studies are essential with different loadings of alumina on titania. However, it is not the primary goal of this investigation. As can be seen from Fig. 3, a sharp rise in the intensity of the Al 2p core level peak with increase in calcination temperature has been observed for both cases. Surface enrichment of alumina particles may be one of the causes for this observation, which will be dealt in the latter paragraphs. In summary, it is evident from Fig. 3 that the Al 2p photoelectron peak depends on the calcination temperature as well as on the coverage by molybdenum oxide on the alumina-titania carrier.

The XPS Mo $3d_{5/2}$ photoelectron peak of MoO_3/Al_2O_3-TiO_2 sample calcined at various temperatures is shown in Fig. 4. As can be noted from this figure, the Mo 3d doublet is well resolved at all temperatures. However, the intensity has been decreased with increase of calcination temperature from 773 to 1073 K. There is a slight increase in the E_b (232.1–232.7 eV) of Mo 3d with increase of calcination temperature. The core level binding energy values indicate that the molybdenum is present in Mo(VI) state and coincides with the literature [28,50]. The slight increase in the E_b with increase of calcination temperature further provides an impression that the dispersed molybdenum may be present in the octahedral Mo(VI) state at lower temperatures and tetrahedral Mo(VI) state due to the formation of $Al_2(MoO_4)_3$ (E_b = 232.7 eV) at higher calcination temperatures [28,49]. It has been reported earlier that a strong interaction between molybdena and alumina favors the presence of more than one type of Mo(VI) species on the alumina surface. Therefore, the XPS Mo 3d doublet was quite broad for MoO_3/Al_2O_3 catalyst [28]. However, Mo species has more uniform geometrical and chemical characteristics on titania surface, which makes the Mo 3d peaks well resolved in the case of MoO_3/TiO_2 catalyst [28]. The structure of surface molybdenum oxide species are primarily isolated, tetrahedrally coordinated at lower loadings, and tend towards polymerized, octahedrally coordinated at higher loadings (near or above monolayer coverage) [14,15,28]. At monolayer coverage, the structure of surface molybdenum oxide species primarily possesses an octahedral coordination on TiO_2 and a mixture of tetrahedral and octahedral coordination on Al_2O_3. As mentioned earlier, in the present investigation a well-resolved Mo 3d doublet peak is observed like the one reported for MoO_3/TiO_2 catalysts. A partial coverage of alumina surface with titania (Al_2O_3:TiO_2 = 1:1.3 mole ratio) lowers the interaction between molybdena and alumina, thereby better resolving the Mo 3d doublet peak similar to those of pure titania-supported catalysts. The XPS atomic ratios described in the next paragraph also support these observations.

The Mo/Al, Mo/Ti, and Ti/Al atomic ratios, as determined by XPS, for the 12 wt.% MoO_3/Al_2O_3-TiO_2 catalyst and for the Al_2O_3-TiO_2 support, respectively, are calculated and shown in Fig. 5 and Table 1. As can be noted from Table 1 and Fig. 5b, the Ti/Al atomic ratio is slightly more for pure support than that of molybdena-doped samples at all calcination temperatures. This observation indicates that molybdenum oxide over-layer has covered the Al_2O_3-TiO_2 support surface. Further, the Ti/Al atomic ratio has been decreased with increase of calcination temperature for both cases. For the pure support, taking into account the fact that the surface free energies of TiO_2 (0.280–0.380 N m^{-1}) are less than those of Al_2O_3 (0.650–0.925 N m^{-1}); the dispersion of titania on alumina is favored according to the thermodynamic rule [51]. The initial surface enrichment of TiO_2 at lower temperatures makes the Ti/Al intensity ratio greater. There could be another explanation also that during precipitation process, microparticles containing titanium previously deposited can act as nucleation centers and cause TiO_2 coverage on Al_2O_3 to take the form of a tower structure [52]. With increase of

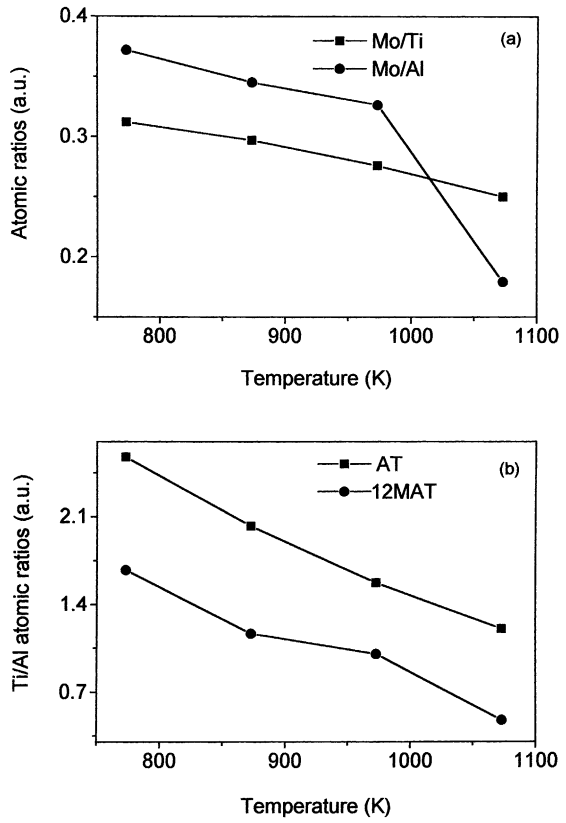

Fig. 5. XPS atomic ratio vs. calcination temperature for the Al_2O_3-TiO_2 (AT) support and MoO_3/Al_2O_3-TiO_2 (12% MAT) catalyst calcined at different temperatures.

calcination temperature, surface enrichment of aluminum particles may occur due to thermally-induced mobility of those particles driven by concentration gradient. In coprecipitation, incorporation of one ion into another oxide matrix is a well-known fact. The ionic radius of octahedrally-coordinated Ti(VI) is 0.605 Å in contrast to the radius of octahedrally-coordinated Al(III) ions which is 0.53 Å [53]. A relatively slight difference between the sizes of these cations suggests that Ti can substitute partially Al in the octahedral sites of alumina during the preparation method. Due to different charges of Ti and Al cations, this substitution requires that close cationic sites should remain partially vacant. For every three Ti cations substituting for Al, one site can remain vacant. The increase in lattice vacancies helps the diffusion of smaller aluminum ions more towards the surface by heat treatment.

As can be seen from Table 1 and Fig. 5a, the Mo/Ti and Mo/Al atomic ratios have exhibited a decreasing trend with increasing calcination temperature. At lower calcination temperatures, the Mo/Al atomic ratio is found to be more than that of Mo/Ti ratio. It is an established fact in the literature that the difference in the surface-free energies between molybdena and alumina (about 0.65 N m^{-1}) is larger than that of molybdena and titania (about 0.3 N m^{-1}) [54]. This means that when both titania and alumina surfaces are bare, molybdena interacts preferentially with alumina portion rather than with titania. It is also well known that isoelectric point or point of zero charge (IEP) of the support oxide also plays a decisive role in the extent of molybdate ion adsorption during preparation. As the isoelectric point of alumina (7.4–8.6) is much higher than that of titania (6.0–6.7), it suggests that the alumina surface should be more positively charged than titania surface and that molybdate adsorption should therefore occur preferentially on the alumina surface [55]. On the other hand, the concentration of anionic surface hydroxyl groups and their distribution on the surface is also the guiding factor for Mo distribution. Both the component oxides are known to have higher concentration of hydroxyl groups on their surfaces, but are uniformly distributed on the TiO_2 surface [56] and in parallel rows on the Al_2O_3 surface [57]. This inherent difference between Al_2O_3 and TiO_2 is reflected in a different distribution of Mo on alumina and titania regions of the mixed oxide support. As Mo is spread more uniformly on TiO_2 than on Al_2O_3 surface, it is expected that size of the monolayer patches may be lower on TiO_2 than on alumina. Ng and Gulari [58] reported formation of multilayer patches and bulk MoO_3 on TiO_2 support when monolayer coverage is exceeded, while for the Mo/Al_2O_3 system multilayer patches were formed even at submonolayer loadings. At higher temperatures, molybdena has less interaction with the support as a result of support sintering, thereby lowering the dispersion on the carrier surface. Another interesting observation from the quantification data is that at 1073 K, dispersion of molybdena was found to be more on titania than on alumina. The occurrence of the well-known and mobile $MoO_2(OH)_2$ species, which are formed by reaction of MoO_3 and H_2O vapor at elevated temperatures [59], would facilitate the diffusion of Mo species into the octahedral interstices of Al_2O_3 enhancing formation and growth

of $Al_2(MoO_4)_3$ compound. The compound formation and its diffusion into the bulk may probably be the reason for the observed decrease in the Mo/Al than Mo/Ti at 1073 K.

4. Conclusions

The following conclusions can be drawn from this study. (a) The core level binding energy of Al 2p increased with increasing calcination temperature. However, the magnitude of increase was slightly more in the case of molybdena-doped samples. This may be due to the removal of negative charge density by exchange of surface hydroxyls between the active component and the support oxide. (b) The presence of more titania than alumina lowers the interaction between molybdena and alumina, and results in a better resolution of Mo 3d doublet. (c) The Ti/Al ratio was found to decrease with increasing calcination temperature, which may be due to thermally-induced surface enrichment of alumina by concentration gradient. (d) The Mo/Al atomic ratio was found to be higher than that of Mo/Ti ratio, and both also decreased with increasing calcination temperature. The difference in the distribution of molybdena over the mixed oxide components is mainly due to various reasons, such as the difference in free energies, isoelectric point, and distribution of hydroxyl groups.

Acknowledgements

EPR thanks the Dirección General de Investigación Científica y Técnica (Spain) for financial support. BC is the recipient of senior research fellowship of the University Grants Commission, New Delhi.

References

[1] H. Knözinger, E. Taglauer, Catalysis, Vol. 10, The Royal Society of Chemistry, Cambridge, 1993, p. 1, and references therein.
[2] H. Topsøe, B.S. Clausen, F.E. Massoth, Hydrotreating Catalysis, Science and Technology, Springer, Berlin, 1996, and references therein.
[3] K. Segawa, I.E. Wachs, in: I.E. Wachs (Ed.), Characterization of Catalytic Materials, Butterworth-Heinemann, Boston, 1992, p. 72.
[4] J.M. Stencel, Raman Spectroscopy for Catalysis, Nostrand Reinhold (Van), New York, 1990, p. 51.
[5] J.R. Bartlett, R.P. Cooney, in: R.J.H. Clark, R.E. Hester (Eds.), Spectroscopy of Inorganic-Based Materials, Wiley, New York, 1987, p. 187.
[6] O.H. Han, C.Y. Lin, N. Sustache, M. McMillan, J.D. Carruthers, K.W. Zilm, G.L. Haller, Appl. Catal. A: Gen. 98 (1993) 195.
[7] G. Mestl, T.K.K. Srinivasan, Catal. Rev.-Sci. Eng. 40 (1998) 451.
[8] D.M. Hercules, J.C. Klein, in: H. Windawi, F.F.L. Ho (Eds.), Applied Electron Spectroscopy for Chemical Analysis, Wiley, New York, 1982.
[9] R. Prins, V.H.J. de Beer, G.A. Somorjai, Catal. Rev.-Sci. Eng. 31 (1989) 1.
[10] H. Topsøe, in: J.P. Bonnelle, B. Delmon, E. Derouane (Eds.), Surface Properties and Catalysis by Non-Metals, Reidel, Dordrecht, 1983, p. 329.
[11] C.C. Williama, J.G. Ekdert, J.M. Jehng, F.D. Hardcastle, I.E. Wachs, J. Phys. Chem. 95 (1991) 8791, and references therein.
[12] C. Martin, I. Martin, V. Rives, P. Malet, J. Catal. 147 (1994) 465.
[13] S. Rajagopal, H.J. Marini, J.A. Marzari, R. Miranda, J. Catal. 147 (1994) 417.
[14] H. Knözinger, in: M.J. Phillips, M. Ternan (Eds.), Proceedings of the 9th International Congress on Catalysis, Calgary, 1988, Vol. 5, The Chemical Society of Canada, Ottawa, 1989, p. 20.
[15] F.E. Massoth, Adv. Catal. 27 (1978) 265, and references therein.
[16] W.K. Hall, in: H.F. Barry, P.C.H. Mitchell (Eds.), Proceedings of the 4th Climax International Conference on Chemistry and Uses of Molybdenum, Climax Molybdenum Co., Ann Arbor, MI, 1982, p. 224.
[17] K. Segawa, T. Soeya, D.S. Kim, Res. Chem. Intermed. 15 (1991) 129.
[18] K. Tanaka, K.I. Tanaka, J. Chem. Soc., Chem. Commun. (1984) 748.
[19] D. Vanhove, S.R. Op, A. Fernández, M. Blanchard, J. Catal. 57 (1979) 253.
[20] V. Harlé, M. Vrinat, J.-P. Scharff, B. Durand, J.-P. Deloume, Appl. Catal. A: Gen. 196 (2000) 261, and references therein.
[21] Z. Wei, Q. Xin, X. Gao, E.L. Sham, P. Grange, B. Delmon, Appl. Catal. 63 (1990) 305.
[22] J. Ramierez, L. Ruiz-Ramierez, L. Cedeno, V. Harlé, M. Vrinat, M. Breysse, Appl. Catal. A: Gen. 93 (1993) 163.
[23] H.M. Matralis, M. Ciardelli, M. Ruwet, P. Grange, J. Catal. 157 (1995) 368.
[24] B.M. Reddy, M.V. Kumar, E.P. Reddy, S. Mehdi, Catal. Lett. 36 (1996) 187.
[25] A. Gutierrez-Alejandro, M. Gonzalez-Cruz, M. Trombetta, G. Busca, J. Ramirez, Microporous Mesoporous Mater. 23 (1998) 265.
[26] P. Concepción, B.M. Reddy, H. Knözinger, Phys. Chem. Chem. Phys. 1 (1999) 3031.
[27] F.E. Massoth, G. Muralidhar, J. Shabtai, J. Catal. 88 (1984) 53.
[28] N.K. Nag, J. Phys. Chem. 91 (1987) 2324, and references therein.

[29] T. Edmonds, P.C.H. Mitchell, J. Catal. 64 (1980) 431.
[30] G. Mestl, N.F.D. Verbruggen, F.C. Lange, B. Tesche, H. Knözinger, Langmuir 12 (1996) 1817.
[31] B.M. Reddy, B. Manohar, E.P. Reddy, Langmuir 9 (1993) 1781.
[32] D. Briggs, M.P. Seah (Eds.), Practical Surface Analysis, Auger and X-Ray Photoelectron Spectroscopy, 2nd Edition, Vol. 1, Wiley, New York, 1990.
[33] D.A. Shirley, Phys. Rev. B 5 (1972) 4709.
[34] A. Savitzky, M.J.E. Golay, Anal. Chem. 36 (1964) 1627.
[35] C.D. Wagner, Discuss Faraday Soc. 60 (1975) 291.
[36] G. Lassaletta, A. Fernández, J.P. Espinós, A.R. González-Elipe, J. Phys. Chem. 99 (1995) 1484.
[37] A.J. Van Hengstun, J.G. Van Ommen, H. Bosch, P.J. Gellings, Appl. Catal. 5 (1983) 207.
[38] D.S. Kim, Y. Kurusu, I.E. Wachs, F.D. Hardcastle, K. Segawa, J. Catal. 120 (1989) 325.
[39] S.W. Weller, Acc Chem. Res. 16 (1983) 101.
[40] D. Goldberg, Rev. Int. Hautes Temper. et Refract. 5 (1968) 181.
[41] G.A. Sawatzky, D. Post, Phys. Rev. B 20 (1979) 1546.
[42] B.R. Strohmeier, D.M. Hercules, J. Phys. Chem. 88 (1984) 4922.
[43] T.L. Barr, C.G. Fries, F. Cariati, J.C.B. Brat, N. Giordano, J. Chem. Soc., Dalton Trans. 1983 (1983) 1825.
[44] B.M. Reddy, I. Ganesh, E.P. Reddy, J. Phys. Chem. 101 (1997) 1769, and references therein.
[45] B.M. Reddy, B. Chowdhury, I. Ganesh, E.P. Reddy, T.C. Rojas, A. Fernández, J. Phys. Chem. B 102 (1998) 10176.
[46] J.A. Mejias, V.M. Jiménez, G. Lassaletta, A. Fernández, J.P. Espinós, A.R. González-Elipe, J. Phys. Chem. 100 (1996) 16255.
[47] B.M. Reddy, V.M. Mastikhin, in: M.J. Phillips, M. Ternan (Eds.), Proceedings of the 9th International Congress on Catalysis, Calgary, 1988, Vol. 1, The Chemical Society of Canada, Ottawa, 1989, p. 82.
[48] C.D. Wagner, H.A. Six, W.T. Jansen, J.A. Tayler, Appl. Surf. Sci. 9 (1981) 203.
[49] D.S. Zingg, L.E. Makovsky, R.E. Tischer, F.R. Brown, D.M. Hercules, J. Phys. Chem. 84 (1980) 2898.
[50] J. Reardon, A.K. Datye, A.G. Sault, J. Catal. 173 (1998) 145.
[51] S.H. Overbury, P.A. Bertrand, G.A. Somorjai, Chem. Rev. 75 (1975) 547.
[52] G.C. Bond, S. Flamrez, L.V. Wijk, Catal. Today 1 (1987) 22.
[53] A.R. West, Solid State Chemistry and its Application, Wiley, New York, 1984 (Chapter 2).
[54] P. Gajardo, A. Mathieux, P. Grange, B. Delmon, Appl. Catal. 3 (1982) 347.
[55] H. Hu, I.E. Wachs, S.R. Bare, J. Phys. Chem. 99 (1995) 10897.
[56] H.P. Boehm, M. Hermann, Z. Anorg. Allg. Chem. 352 (1976) 156.
[57] H. Knözinger, P. Ratnasamy, Catal. Rev.-Sci. Eng. 17 (1978) 31.
[58] K.Y.S. Ng, E. Gulari, J. Catal. 92 (1985) 340.
[59] O. Glemser, H.G. Wendlandt, Angew. Chem. 75 (1963) 949.